

# Four Specific Hapten Conformations Dominating Antibody Specificity: Quantitative Structure–Activity Relationship Analysis for Quinolone Immunoassay

Jiahong Chen,<sup>†,‡</sup> Lanteng Wang,<sup>†,‡</sup> Lanlan Lu,<sup>†</sup> Xing Shen,<sup>†</sup> Xin-an Huang,<sup>§</sup> Yingju Liu,<sup>||</sup> Xiulan Sun,<sup>⊥</sup> Zhanhui Wang,<sup>#</sup> Sergei Alexandrovich Eremin,<sup>∇,○</sup> Yuanming Sun,<sup>†</sup> Zhenlin Xu,<sup>†</sup> and Hongtao Lei<sup>\*,†,⊥</sup>

<sup>†</sup>Guangdong Provincial Key Laboratory of Food Quality and Safety and <sup>||</sup>Department of Applied Chemistry, College of Materials and Energy, South China Agricultural University, Guangzhou 510642, China

<sup>§</sup>Tropical Medicine Institute & South China Chinese Medicine Collaborative Innovation Center, Guangzhou University of Chinese Medicine, Guangzhou 510405, China

<sup>⊥</sup>State Key Laboratory of Food Science and Technology, School of Food Science of Jiangnan University, Wuxi, Jiangsu 214122, China

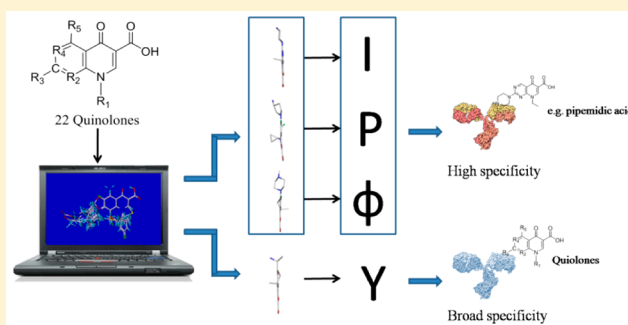
<sup>#</sup>Department of Veterinary Pharmacology and Toxicology, College of Veterinary Medicine, China Agricultural University, Beijing 100094, China

<sup>∇</sup>Faculty of Chemistry, M.V. Lomonosov Moscow State University, Leninskie gory 1, Building 3, 119991 Moscow, Russia

<sup>○</sup>A.N. Bach Institute of Biochemistry, Research Center of Biotechnology of the Russian Academy of Sciences, Moscow, Russia

## Supporting Information

**ABSTRACT:** Antibody-based immunoassay methods have been important tools for monitoring drug residues in animal foods. However, because of limited knowledge about the quantitative structure–activity relationships between a hapten and its resultant antibody specificity, antibody production with the desired specificity is still a huge challenge. In this study, the three-dimensional quantitative structure–activity relationship (3D QSAR) was analyzed in accordance with the cross-reactivity of quinolone drugs reacting with the antibody raised by pipemidic acid as the immunizing hapten and compared with the reported cross-reactivity data and their hapten structures. It was found that the specificity of a quinolone antibody was strongly related to the conformation of the hapten used and that hapten conformations shaped like the letters “I”, “P”, and “Φ” were essential for the desired high specificity with low cross-reactivity, but that the hapten conformation shaped like the letter “Y” led to an antibody with broad specificity and high cross-reactivity. Almost all of the antibodies against quinolones could result from these four hapten conformations. It was first found that the concrete conformations dominated the specificity of the antibody to quinolone, which will be of significance for the accurate hapten design, predictable antibody specificity, and better understanding the recognition mechanism between haptens and the antibodies for immunoassays.



Quinolones are a class of antimicrobial drugs that are widely used in the prevention and treatment of animal diseases. However, their residues in animal foods have raised a series of health issues, including skin reactions, phototoxicity, and hyperglycemia.<sup>1–3</sup> To effectively monitor quinolone abuse in animal-derived food products, it is important to develop a rapid screening method for monitoring quinolone residues. Compared with the traditional instrumental methods,<sup>4–8</sup> immunoassays relying on antigen–antibody interactions are favored by analytical chemists because of their convenient manipulation, simple sample treatment, low costs, and easy automation. Some immunoassays have been developed for the detection of quinolone residues.<sup>9–11</sup>

It is well-known that an antibody with the desired broad or high specificity (high or low cross-reactivity) is crucial to

develop an immunoassay.<sup>12</sup> High specificity means low cross-reactivity to structurally related compounds,<sup>13,14</sup> which is traditionally favored by a single analyte analysis in one test. On the contrary, broad specificity means that the high cross-reactivity to structurally related compounds is useful for the monitoring of series of compounds to complete a multianalyte analysis in one test.<sup>15</sup> Now, the broad-specificity, multianalyte recognition in one assay seems to be a focus of antibody production and immunoassay development for quinolone drugs.<sup>16–18</sup> There have been a few reports of the broad specificity of quinolone antibodies based on molecular modeling.

**Received:** March 17, 2017

**Accepted:** May 17, 2017

**Published:** May 17, 2017



Wang et al. developed a generic immunoassay using ciprofloxacin antibodies for 12 fluoroquinolone antibiotics, and the obtained cross-reactivity data showed that the ethyl group of the piperazinyl ring exerted a limited effect on antibody binding but appeared to be important during antibody production.<sup>18</sup> In a previous study, we employed pazufloxacin as the hapten to produce a broad specific antibody recognizing 23 quinolones.<sup>19</sup> We found that the quinolones could interact with the antibody in different binding positions and that cross-reactivity was mainly positively correlated with a bulky substructure containing an electronegative atom at position 7, whereas it was negatively associated with the presence of a large bulky substructure at position 1 of the quinolones.<sup>19</sup> Even though the topological properties of haptens provide a rich body of structural information that could be helpful for understanding the specificities of antibodies,<sup>19</sup> the reasonable prediction and design of the resultant antibody specificity are still great challenges because of the unclear structure–activity relationship and limited knowledge about the recognition mechanism.<sup>19</sup>

In this study, pipemidic acid, a quinolone drug with a flat conformation shaped like the letter “I” at position 7, was used as the hapten to produce a polyclonal antibody, and a highly sensitive competitive indirect enzyme-linked immunosorbent assay (ciELISA) was successfully constructed in a heterologous coating format. Using comparative molecular field analysis (CoMFA) based on the obtained cross-reactivity of the antibody raised by pipemidic acid, a three-dimensional quantitative structure–activity relationship (3D QSAR) was constructed among quinolone hapten structures and the specificity of the pipemidic acid antibody. Moreover, through a comparison with the reported cross-reactivity data and the structure of typical quinolone haptens including cinafloxacin, ofloxacin, pazufloxacin, and ciprofloxacin, the optimal hapten conformations for

the corresponding antibody specificity were investigated for the first time.

## EXPERIMENTAL SECTION

**Reagents.** Pipemidic acid, 3,3',5,5'-tetramethylbenzidine (TMB), bovine serum albumin (BSA), ovalbumin (OVA), complete and incomplete Freund's adjuvants, 1-(3-(dimethylamino)propyl)-3-ethylcarbodiimide hydrochloride (EDC), Tween-20, and *N,N*-dimethylformamide (DMF) were purchased from Sigma (St. Louis, MO). HRP-conjugated goat-antirabbit immunoglobulin G (IgG) was obtained from Boster Biotech Corporation Limited. (Wuhan, China). Rufloxacin, prulifloxacin, norfloxacin, pefloxacin, enrofloxacin, oxolinic acid, racemic ofloxacin, ciprofloxacin, lomefloxacin, danofloxacin, garenoxacin, pazufloxacin, cinafloxacin, gatifloxacin, marbofloxacin, difloxacin, sarafloxacin, sparfloxacin, and tosufloxacin were purchased from Veterinary Medicine Supervisory Institute of China (Beijing, China). (*S*)-(-)-ofloxacin and (*R*)-(+)-ofloxacin were purchased from Daicel Chiral Technologies Company (Figure 1). All of the chemicals and organic solvents, which were of analytical grade or better, were obtained from a local chemical supplier (Yunhui Trade Co., Ltd., Guangzhou, China). The coating buffer, washing solution, blocking solution, substrate buffer, stopping reagent, and TMB solution used in this study were prepared as in previous work in our laboratory.<sup>20</sup> Standard stock solutions (1 mg/mL) were prepared by dissolving the appropriate amount of each standard in 0.03 mol/L sodium hydroxide solution and holding the solutions at 4 °C until use. Working standard solutions (0.038, 0.31, 2.44, 19.53, 156.25, 1250, and 10000 ng/mL) were prepared by diluting the stock solution in phosphate-buffered saline with 0.1% Tween-20 (PBST).

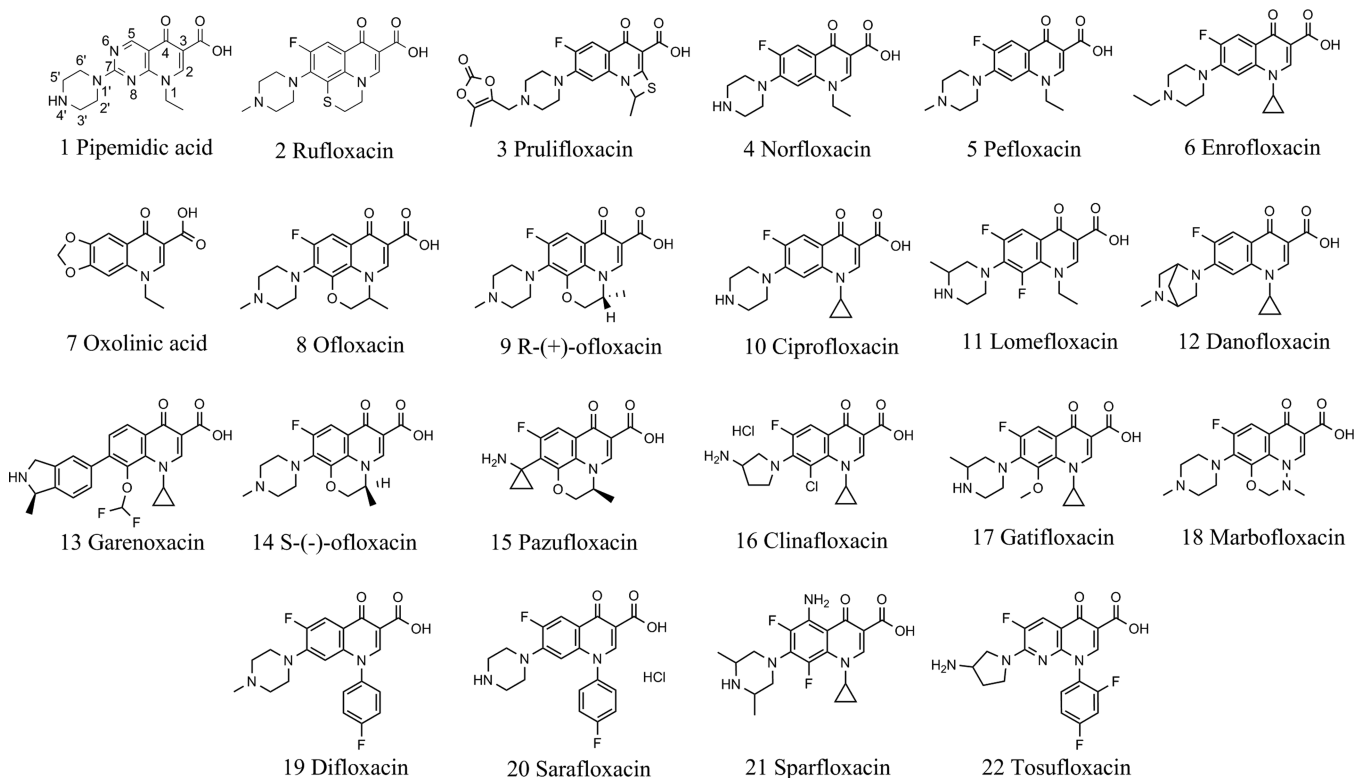


Figure 1. Structures of quinolones.

**Instruments.** UV–visible absorption measurements were performed on a UV-3010 spectrophotometer (Hitachi, Tokyo, Japan). ELISA plates were washed with a DEM-3 microtiter plate washer (Tuopu, China). Absorbance was measured at a wavelength of 450 nm using a Multiskan MK3 microplate reader (Thermo Labsystems, USA).

**Preparation of Hapten–Protein Conjugates.** Pipemidic acid was coupled to BSA through EDC for the immunogen, and both pipemidic acid and quinolone drugs (norfloxacin–OVA, pazufloxacin–OVA, ciprofloxacin–OVA, gatifloxacin–OVA, lomefloxacin–OVA, sarafloxacin–OVA, and garenoxacin–OVA) were coupled with OVA through EDC for use of the coating antigens according to previous work with modifications.<sup>21</sup>

**Antibody Production.** Animal treatments were conducted in accordance with the guidelines of the Chinese Association for Laboratory Animal Sciences. Two New Zealand rabbits (1.5–2.0 kg), supplied by the Guangdong Medical Laboratory Animal Center, were immunized using pipemidic acid–BSA as the immunogen to generate the polyclonal antibody against pipemidic acid according to our previous work with modifications.<sup>20</sup> The obtained antisera from rabbits were purified by caprylic acid-saturated ammonium sulfate precipitation, and the purity was confirmed by sodium dodecyl sulfate–polyacrylamide gel electrophoresis (SDS–PAGE). Then, the antisera were divided into aliquots, labeled, and stored at –20 °C until use.<sup>22</sup>

**ELISA Procedure.** The ELISA was established on the basis of the common procedure of competitive indirect enzyme-linked immunosorbent assay (ciELISA).<sup>20</sup> Calibration curves were obtained by plotting the normalized signal  $B/B_0$  against the logarithm of the analyte concentration. The logarithm of the pipemidic acid concentration served as the  $X$  axis, whereas  $B/B_0$  (where  $B$  is the average absorbance of the wells in the presence of a competitor and  $B_0$  is the average absorbance of the well without analyte) served as the  $Y$  axis. The 50% inhibition values ( $IC_{50}$ ) were obtained using a four-parameter logistic equation that was used to fit the sigmoidal curve using OriginPro 8.5 software (OriginLab Corporation, Northampton, MA).<sup>23</sup> The equation was as follows

$$Y = \frac{(A - D)}{[1 + (X/C)^E]} + D$$

where  $A$  is the maximum response at high asymptotes of the curve,  $D$  is the minimum response at low asymptotes of the curve,  $C$  is the concentration of the analyte that resulted in 50% inhibition, and  $E$  is the slope of sigmoidal curve. The limit of detection (LOD) was defined as the concentration of analyte that provided 10% inhibition ( $IC_{10}$ ).<sup>24</sup> The dynamic working range was defined as the lower and upper concentrations that provided 20–80% inhibition.<sup>25</sup>

**Specificity.** The specificity of the antibody was evaluated by measuring the cross-reactivity (CR) using a group of structurally related quinolone drugs. Twenty-two compounds were selected for this test (Figure 1), and the obtained  $IC_{50}$  values were used to calculate cross-reactivities as follows

$$CR (\%) = \left[ \frac{IC_{50}(\text{pipemidic acid})}{IC_{50}(\text{structurally related quinolone drugs})} \right] \times 100\%$$

**QSAR.** CoMFA for Pipemidic Acid Immunoassay. Molecular modeling was conducted using the SYBYL-X 2.1 program package. The 22 molecules in the data set were constructed using the “SKETCH” option function; then, they

were energy-minimized using the Powell method with the MMFF94 force field and MMFF94 charges. The criteria for termination and the maximum number of iterations were set to be 0.005 kcal/(mol Å) and 1000, respectively. The other parameters were the defaults. Molecular alignment was performed using pipemidic acid as the template molecule and its C-4a, C-5, N-8, and C-8a unit as the common core structure. Pipemidic acid, prulifloxacin, rifloxacin, norfloxacin, pefloxacin, enrofloxacin, lomefloxacin, danofloxacin, garenoxacin, (S)-(–)-ofloxacin, clinafloxacin, gatifloxacin, marbofloxacin, difloxacin, sarafloxacin, sparfloxacin, and tosufloxacin were classified into the training set, and oxolinic acid, (R)-(+)-ofloxacin, ciprofloxacin, and pazufloxacin were treated as the test set. The converted  $pIC_{50}$  ( $-\log IC_{50}$ ) values were used in the analysis.

CoMFA steric and electrostatic interaction fields of each molecule were calculated on a 3D cubic lattice. An  $sp^3$  carbon probe atom with a van der Waals radius of 1.52 Å and charge of +1 was used to generate the steric and electrostatic field energies. The cross-validated correlation coefficient,  $R^2$  ( $q^2$ ), and the optimum number of components (ONC) were obtained using the partial least-squares (PLS) method with the leave-one-out (LOO) option. Using the obtained optimum numbers of components, the final non-cross-validated model was created. Except for use of the MMFF94 charges, the other parameters or options of the CoMFA were the defaults.

**Conformation Comparison Analysis.** Previously, we raised a clinafloxacin polyclonal antibody and developed a rapid, specific immunoassay for clinafloxacin.<sup>21</sup> In this work, the converted  $pIC_{50}$  ( $-\log IC_{50}$ ) values for the cross-reactivity data of clinafloxacin were directly used for molecular modeling. The molecular alignment was carried out using clinafloxacin as the template molecule and its C-4a, C-5, N-8, and C-8a atoms as the common core structure. Clinafloxacin, gatifloxacin, ciprofloxacin, (S)-(–)-ofloxacin, rifloxacin, enrofloxacin, marbofloxacin, lomefloxacin, prulifloxacin, pefloxacin, nalidixic acid, tosufloxacin, and difloxacin were classified into the training set, and danofloxacin, (R)-(+)-ofloxacin, sparfloxacin, and sarafloxacin were treated as the test set. Molecular modeling was conducted using the same method and parameters as above. The comparative molecular field analyses of other quinolones, including pazufloxacin, ciprofloxacin, and ofloxacin, were reported in the literature and were used for discussion in this study.<sup>18,26,27</sup>

## RESULTS AND DISCUSSION

**Immunoreagent Preparation.** The pipemidic acid bearing a carboxylic acid group at the end of the spacer was covalently coupled with a carrier protein (BSA or OVA) by the direct EDC method. UV spectra were measured to ensure the successful conjugation. Figure S1 shows the UV spectra of BSA, OVA, pipemidic acid, pipemidic acid–BSA and pipemidic acid–OVA. BSA/OVA showed a characteristic absorption peak at 280 nm, whereas pipemidic acid exhibited a peak at 332 nm. The absorption spectra of pipemidic acid–BSA/OVA conjugates contained absorption peaks of both pipemidic acid and BSA/OVA, but with somewhat of a blue shift. This indicates that the coupling of pipemidic acid to BSA and OVA was successful.<sup>28</sup> Similar results were obtained with other quinolone drug–OVA conjugates (data not shown). The SDS–PAGE results showed that the purified pipemidic acid antibody had a heavy chain observed at 50 kDa and a light chain at about 25 kDa. There was no superfluous band (Figure S2). Thus, the purified antibody was ideal for further investigation.

**Optimization of ciELISA.** To obtain the optimal sensitivity of ciELISA, the concentration of coating antigen and the antibody dilution time were optimized to obtain a maximum absorbance ( $A_{\max}$ ) for the zero standard concentration (blank) in the range of 1.0–1.5 and the best sensitivity (minimum  $IC_{50}$  value).<sup>29</sup>

For homologous assay format (pipemidic acid–OVA for the use of the coating antigen), a poor binding affinity with a low inhibition rate of 48.05% was obtained. In addition, the standard curve for pipemidic acid (Figure 2) was constructed in

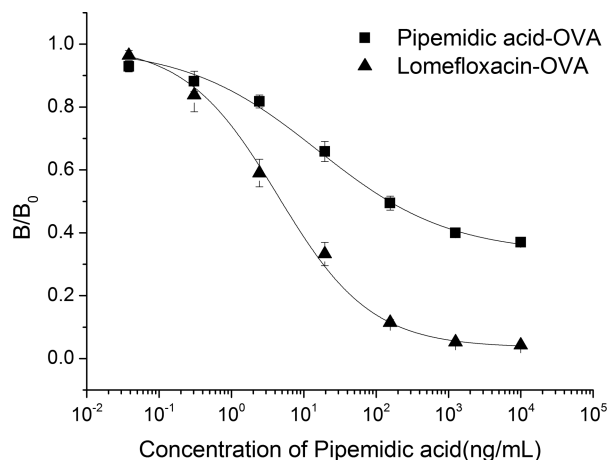


**Figure 2.** ciELISA calibration curves for pipemidic acid with different coating antigens. Each point represents mean  $\pm$  standard deviation of three replicates.

the concentration range from 6.53 to 144.87 ng/mL, and the value of the LOD at 10% inhibition was within 2.6 ng/mL. These results indicate that the sensitivity was 14.4 times lower than that of the ultraperformance liquid chromatography–tandem mass spectrometry (UPLC–MS/MS) method<sup>7</sup> and that the inhibition rate (48.05%) was undesirable, which failed to meet the purpose of this study.

To obtain better sensitivity, a series of coating antigens (norfloxacin–OVA, pazufloxacin–OVA, ciprofloxacin–OVA, gatifloxacin–OVA, lomefloxacin–OVA, sarafloxacin–OVA, and garenoxacin–OVA) were compared at the same coating concentration (1  $\mu$ g/mL) (Table S1). Surprisingly, although the homologous assay format demonstrated a better titer (titer = 32000) than any of the heterogeneous formats (norfloxacin–OVA, pazufloxacin–OVA, ciprofloxacin–OVA, gatifloxacin–OVA, lomefloxacin–OVA, sarafloxacin–OVA, and garenoxacin–OVA for the use of the coating antigens),

it was found that lomefloxacin–OVA showed the highest inhibition rate (86.7%) with a titer of 8000.

The calibration curves for pipemidic acid in the homologous and heterogeneous assay formats were constructed (Figure 2). Compared with the  $IC_{50}$  (30.76 ng/mL) and LOD (2.64 ng/mL) for the homologous assay format (Table S1 and Figure 2), the  $IC_{50}$  and LOD for the heterogeneous assay format (with lomefloxacin–OVA as the coating antigen) were 5.99 ng/mL and 0.31 ng/mL, respectively, indicating that the sensitivity was better than that of the homologous combination and that of the reported physicochemical method.<sup>7</sup> As a result, the combination of the pipemidic acid antibody and lomefloxacin–OVA was used for further investigation because of its improved sensitivity.

**Specificity.** The cross-reactivities of 22 types of quinolones were determined using the developed ELISA with pipemidic acid as the reference compound. Except for rifloxacin and prulifloxacin, the cross-reactivity values of other quinolones were found to be lower than 15% (Table 1). Only 9% of the quinolones in this study displayed cross-reactivities that were greater than 15%; thus, these results can be regarded as indicating the high specificity of the pipemidic acid antibody.

Generally, high cross-reactivities of haptens can be directly ascribed to similarities in their molecular structures, and low cross-reactivities are possibly related to the structural differences of the cross-reactants.<sup>30</sup> In this study, norfloxacin was confirmed to be a good hapten candidate resulting in a broad-specificity antibody that could recognize 13 quinolones.<sup>31</sup> The structural differences between norfloxacin and pipemidic acid occur at positions 6 and 8, where norfloxacin contains a carbon atom at position 6 and a C–F group at position 8, whereas pipemidic acid contains nitrogen atoms at both of these locations. Such differences seem to be a minimal, but the cross-reactivities of norfloxacin and pipemidic acid were found to be significantly different (14.1% for norfloxacin, 100% for pipemidic acid). This suggests that positions 6 and 8 are likely crucial to the desired hapten conformation for antibody recognizing. Moreover, the structures of rifloxacin and ofloxacin are similar except for the ring formed by the group at positions 1 and 8. This implies that the ring also plays an important role in hapten–antibody binding. Additionally, compared with the structure of pipemidic acid, difloxacin contained one supplemental benzene ring at position 1; however, the cross-reactivity of difloxacin dropped dramatically from CR 100% for pipemidic acid to CR 0.5%. Moreover, the cross-reactivities of sarafloxacin (CR = 0.3%) and tosufloxacin (CR = 0.3%) were also very low because of the benzene ring added at position 1. These dramatic changes in cross-reactivity indicate the importance of the groups at

**Table 1.** Cross-Reactivities of Pipemidic Acid and 22 Quinolone Drugs Based on Coating Antigen Lomefloxacin–OVA

name	$IC_{50}$ (nmol/mL)	CR (%)	name	$IC_{50}$ (nmol/mL)	CR (%)
pipemidic acid	0.0076	100.0	danofloxacin	0.21	3.6
rufloxacin	0.026	29.5	garenoxacin	0.23	3.3
prulifloxacin	0.026	28.8	(S)-(–)-ofloxacin	0.26	2.9
norfloxacin	0.054	14.1	pazufloxacin	0.27	2.8
pefloxacin	0.056	13.4	clinafloxacin	0.49	1.5
enrofloxacin	0.071	10.7	gatifloxacin	0.50	1.5
oxolinic acid	0.082	9.2	marbofloxacin	0.96	0.8
ofloxacin	0.090	8.4	difloxacin	1.49	0.5
(R)-(+)-ofloxacin	0.10	7.3	sarafloxacin	2.32	0.3
ciprofloxacin	0.14	5.4	sparfloxacin	2.53	0.3
lomefloxacin	0.21	3.7	tosufloxacin	2.91	0.3



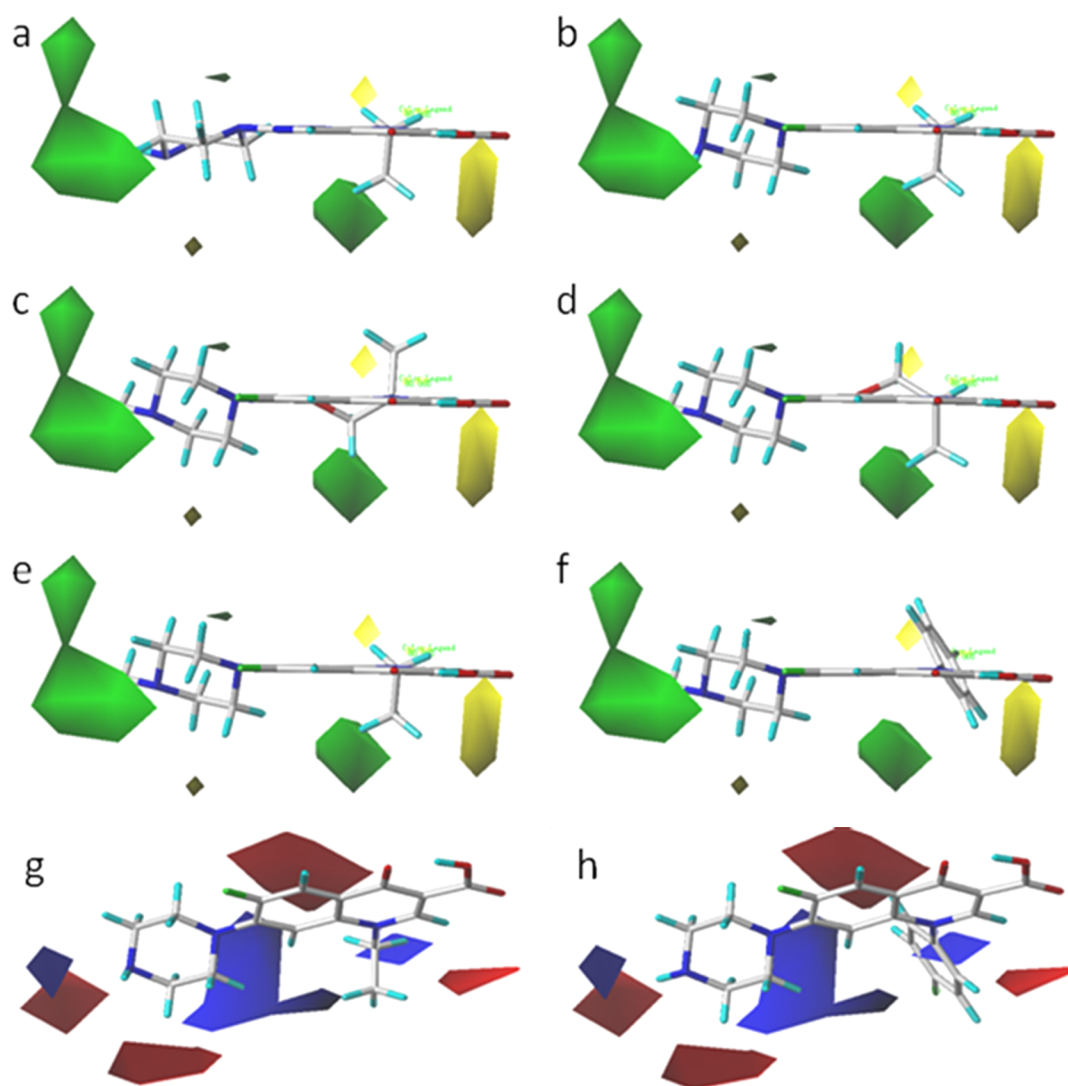


**Figure 3.** CoMFA contour maps of pipemidic acid. (a–f) CoMFA steric contour maps together with (a) embedded pipemidic acid, (b) embedded norfloxacin, (c) embedded (R)-(+)-ofloxacin, (d) embedded (S)-(-)-ofloxacin, (e) embedded pefloxacin, and (f) embedded difloxacin. (g,h) CoMFA electrostatic contour maps together with (g) embedded norfloxacin and (h) embedded sarafloxacin. The energies of all fields were calculated with the weight of the standard deviation and the coefficient. Green, yellow, blue, and red contours represent steric bulk desirable, steric bulk undesirable, positive charge desirable, and negative charge desirable, respectively.

positions 1, 6, and 8 for a desired binding conformation. To better understand the high specificity of the obtained pipemidic acid antibody, CoMFA was used for further investigation.























**CoMFA Analysis.** The CoMFA models exhibited rational  $q^2$  values greater than 0.5, and the *S* and *E* fields offered 58.2% and 41.8% contributions, respectively, to the affinity (Table S2). The  $\text{pIC}_{50}$  values of the molecules in the test set were perfectly predicted in the CoMFA model (Figure S3).

The contour maps reflect the desired/undesired steric/electrostatic features for molecular binding affinity in the CoMFA model, in which the green and yellow contours represent the favorable and unfavorable steric regions, respectively, whereas the blue and red contours represent the favorable and unfavorable electropositive regions, respectively. The piperazine ring at position 7 was nearly in the same plane with the basic structure, 1,4-dihydro-4-oxo-3-quinolinecarboxylic acid, shared by almost all quinolones (Figure 3a), and the conformation of pipemidic acid was shaped like the letter I. Thus, from the perspective of looking down at the molecule, the piperazine ring formed a flat antibody binding cavity that could not accommodate a large group.

In addition, the green contour was near position 4' of pipemidic acid (Figure 3a), which implies that the antibody could not recognize the groups at both sides of position 7. However, the piperazine ring at position 7 of norfloxacin was almost perpendicular to the basic structure (Figure 3b). As a result, to accommodate a large group, it seems to be essential for the hapten to have a large antibody binding cavity at this position. The piperazine ring at position 7 in other quinolones was also essentially perpendicular to the basic structure and was consistent with norfloxacin (Figure 3c–f). These features could constitute the main reason that the resultant antibody against pipemidic acid exhibited low cross-reactivity to quinolones.

The hydrogen atom at the oxazine ring of (S)-(-)-ofloxacin interacted with the little yellow contour, and the methyl group was near the large yellow contour, whereas the hydrogen atom at the oxazine ring of (R)-(+)-ofloxacin interacted with the green contours, and the methyl group deviated from the little yellow contour because of their opposite conformations (Figure 3c,d). This could be the reason that (S)-(-)-ofloxacin (experimental  $\text{pIC}_{50} = 9.585$ ) showed a lower binding activity

**Table 2.** Models of the Minimum-Energy Conformations of the Quinolones from the Immunoassay for Pipemidic Acid and for Clinafloxacin<sup>c</sup>

Shape	Characteristic	Models of the minimum energy conformations of the quinolones			
I	High-specificity <sup>a</sup>				
P	High-specificity				
Φ	High-specificity				
					
					
					
Y	Broad-specificity <sup>b</sup>				

<sup>a</sup>High specificity means less than 3 types of structurally related quinolones whose cross-reactivity values were over 15%. <sup>b</sup>Broad specificity means that most of the structurally related quinolones had cross-reactivity values of over 15%. <sup>c</sup>Elements represented as follows: oxygen, red; nitrogen, navy blue; hydrogen, light blue; fluorine, green; carbon, white; sulfur, yellow.

to the pipemidic acid antibody than that of (R)-(+)-ofloxacin (experimental  $\text{pIC}_{50} = 10.000$ ) (Table S3). Comparison of the conformation of (S)-(-)-ofloxacin with that of norfloxacin shows that the group at position 8 in (S)-(-)-ofloxacin is larger and closer to the yellow contours than that of norfloxacin, which could be ascribed to the lower activity of (S)-(-)-ofloxacin (experimental  $\text{pIC}_{50} = 9.585$ ) (Figure 3b,d). In addition, from a comparison of the CoMFA maps of pefloxacin and difloxacin (Figure 3e,f), the yellow contours near the benzene ring of difloxacin indicated that the bulky group at position 1 decreased the binding activity; therefore, the activities of difloxacin (experimental  $\text{pIC}_{50} = 8.827$ ) were lower than those of pefloxacin (experimental  $\text{pIC}_{50} = 10.252$ ) (Table S3).

In addition to the major contribution of the steric field, the electrostatic field also plays an important role in the quinolone–antibody binding conformation (Figure 3g,h). The difference between norfloxacin and sarafloxacin was the group at position 1, and the group interacted with the blue contour of a rhombus. However, the electronegative fluorine atom of sarafloxacin was near these regions, which additionally led to a lower binding activity for sarafloxacin. This indicates that electronegative groups at position 1 decreased the binding activity, which was consistent with the conclusions based on the steric effect above.

**Conformation Comparison Analysis.** Table 2 shows 22 types of models of the minimum-energy conformations of the quinolones from the immunoassay for pipemidic acid in this study and the previously reported immunoassay for clinafloxacin.<sup>21</sup> These models were divided into four groups in accordance with their conformational features at the minimum energy. The first group contained pipemidic acid, nalidixic acid, and oxolinic acid, and their conformations were shaped like the letter I. The second group contained clinafloxacin, danofloxacin, and tosufloxacin, and their conformations were shaped like a letter “P”. The third group contained difloxacin, enrofloxacin, gatifloxacin, lomefloxacin, pefloxacin, rufloxacin, (R)-(+)-ofloxacin, (S)-(-)-ofloxacin,

garenoxacin, prulifloxacin, sparfloxacin, and marbofloxacin, and their conformations were shaped like the Greek letter “Φ”. The fourth group contained ciprofloxacin, norfloxacin, pazufloxacin, and sarafloxacin, and their conformations formed a “Y” shape (or a lollipop).

In the first group, the conformation features of nalidixic acid and oxolinic acid were also shaped like the letter I and were consistent with pipemidic acid. Thus, the antibody derived from nalidixic acid or oxolinic acid as a hapten could be of high specificity.

In the second group, CoMFA was used for the further investigation of the clinafloxacin immunoassay. The CoMFA models exhibited a rational  $q^2$  value of 0.587, and the *S* and *E* fields offered 53.4% and 46.6% contributions, respectively, to the affinity (Table S2). The  $\text{pIC}_{50}$  values of the molecules in the test set were perfectly predicted (Figure S3). Therefore, the contour analysis of the model was further carried out.

The group at position 7 of clinafloxacin was on the side of the basic structure plane, and the conformation of clinafloxacin was shaped like the letter “P” (Figure 4a). In addition, the green contour was near the amino group at position 3' in clinafloxacin (Figure 4a). This implies that the antibody to clinafloxacin could not recognize the group on the side near position 5'. However, the piperazine ring at position 7 in ciprofloxacin was basically perpendicular to the basic structure (Figure 4b). Furthermore, other quinolones with the piperazine ring at position 7 were also basically perpendicular to the basic structure and were consistent with that of ciprofloxacin (Figure 4c–f). Moreover, the amino group and five-membered ring at position 7 seemed to form a small antibody binding cavity that would not accommodate a large group. For example, a piperazine ring is a large group that could not be accommodated in the small antibody binding cavity formed by the amino group and five-membered ring of clinafloxacin. However, ciprofloxacin shaped like a Y and the piperazine ring in ciprofloxacin could form a larger antibody binding cavity, and thus the larger antibody binding cavity should contribute to the broad specificity of the corresponding antibody to ciprofloxacin, and in turn, the high specificity of clinafloxacin antibody would

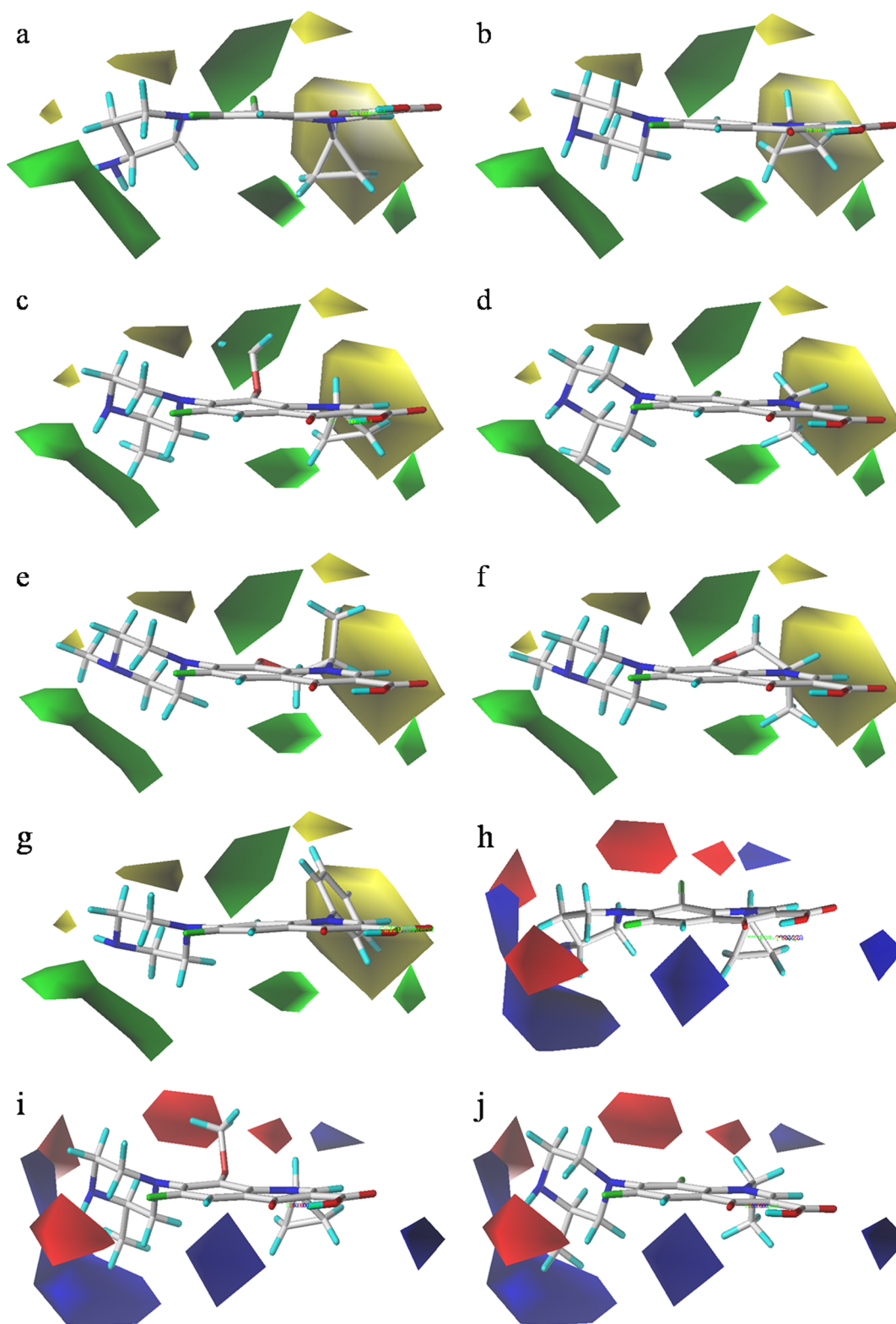


**Figure 4.** CoMFA contour maps of clinafloxacin. (a–f) CoMFA steric contour maps together with (a) embedded clinafloxacin, (b) embedded ciprofloxacin, (c) embedded gatifloxacin, (d) embedded lomefloxacin, (e) embedded (*R*)-(+)-ofloxacin, (f) embedded (*S*)-(–)-ofloxacin, and (g) embedded sarafloxacin. (h–j) CoMFA electrostatic contour maps together with (h) embedded clinafloxacin, (i) embedded gatifloxacin, and (j) embedded lomefloxacin. The energies of all fields were calculated with the weight of the standard deviation and the coefficient. Green, yellow, blue, and red contours represent steric bulk desirable, steric bulk undesirable, positive charge desirable, and negative charge desirable, respectively.

also be understandable. The previous study of clinafloxacin also showed that all of the CRs for structurally related quinolones were lower than 15% (Table S5).<sup>21</sup>

In addition, when comparing the contour maps of gatifloxacin, lomefloxacin, and (*S*)-(–)-ofloxacin (Figure 4c,d,f), we found that the group at position 8 of gatifloxacin was larger and closer

to the green contour than for that in (S)-(-)-ofloxacin. However, the group at position 8 in (S)-(-)-ofloxacin was larger and closer than those in lomefloxacin. This trend can be ascribed to the highest activity of gatifloxacin (experimental  $\text{pIC}_{50} = 6.076$ ), followed by (S)-(-)-ofloxacin (experimental  $\text{pIC}_{50} = 5.440$ ), and lomefloxacin (experimental  $\text{pIC}_{50} = 4.828$ ) (Table S4).

The green contour at the bottom of the map interacted with the methyl at the oxazine ring of (S)-(-)-ofloxacin, whereas the methyl at the oxazine ring of (R)-(+)-ofloxacin was brought near the yellow contour in the upper portion of the map because of their opposite conformations (Figure 4e,f). This reveals the mechanism that (S)-(-)-ofloxacin had a higher binding affinity than (R)-(+)-ofloxacin. For the antibody distinguishing the chiral isomer of quinolones, the bulky group near the green contour at position 8 was found to play a critical role. From a comparison of the CoMFA maps of sarafloxacin and ciprofloxacin, the yellow contours near the benzene ring of sarafloxacin indicate that the bulky group at position 1 decreased the binding activity (Figure 4b,g). Therefore, the activities of sarafloxacin (experimental  $\text{pIC}_{50} = 4.628$ ) were lower than those of ciprofloxacin (experimental  $\text{pIC}_{50} = 5.640$ ) (Table S4). Because the yellow contours are near the benzene ring of sarafloxacin, it is understandable that the activity of sarafloxacin (experimental  $\text{pIC}_{50} = 4.628$ ) was lower, and the predicted  $\text{pIC}_{50}$  value of sarafloxacin in the test set was lower than the experimental value (Table S4).

The electrostatic contour maps also reflected the molecular binding affinity in the CoMFA model (Figure 4). The amino group at position 7 in clinafloxacin near the blue contour was a strong electron-donating group, whereas the groups of gatifloxacin and lomefloxacin were weak electron-donating groups. As a result, the binding activity of gatifloxacin or lomefloxacin was much lower than that of clinafloxacin, which is consistent with the steric results described above. The conformations of danofloxacin and tosufloxacin in the second group were also shaped like the letter P, and as a result, similarly to clinafloxacin, their antibodies also would show high-specificity as clinafloxacin. This was confirmed in a previous study using antidanofloxacin antibody (Table S5).<sup>32</sup> The conformation of tosufloxacin demonstrated a high similarity to that of clinafloxacin and could be a suitable hapten for the production of highly specific antibody.

The third group consisted of 12 types of quinolones in this study, all shaped like the Greek letter “ $\Phi$ ”, and it could accordingly be predicted that their antibodies would be highly specific; this was also confirmed by experiments (Table 2 and Table S5).<sup>10,11,27,33–37</sup> For example, ofloxacin contains a substituent on the piperazine ring at position 7, and a previous QSAR study showed that the green contour was near the substituent, whereas two yellow contours were distributed on the two sides of the piperazine ring.<sup>27</sup> This implies that the antibody could not recognize quinolones without a substituent on the piperazine ring or with a substituent on another site of piperazine ring. In addition, the experimental cross-reactivities had already confirmed that only rufloxacin, garenoxacin, and marbofloxacin had high cross-reactivity values (cross-reactivity >15%).<sup>27</sup> Therefore, it can be concluded that hapten quinolones shaped like an I, P, or  $\Phi$  would result in an antibody with low cross-reactivity and high specificity.

In the fourth group (Table 2), unlike the structures shaped like the letters I, P, and  $\Phi$ , all of the proposed compounds were shaped like the letter Y or a lollipop. Their conformations could

be predicted to produce a large antibody binding cavity to accommodate the piperazinyl group at position 7 (Table 2). For example, pazufloxacin contained a 1-aminocyclopropyl group at position 7 but not a piperazinyl group shared by many quinolones. Both the amino and cyclopropyl groups around position 7 of pazufloxacin formed a Y shape or a lollipop, and the green contour also lay on both sides of position 7.<sup>26</sup> This implies that the resultant antibody to pazufloxacin would broadly recognize other quinolones. In fact, the experimentally identified pazufloxacin antibody with a high sensitivity and broad specificity could recognize 24 quinolones, as expected (Table S5).<sup>26</sup> This is a broad specificity, but not a high specificity, because pazufloxacin is not shaped like any of the three conformations I, P, or  $\Phi$ .

Ciprofloxacin is another good example for confirming the three essential conformations for a high specificity.<sup>18</sup> The piperazine ring at position 7 in ciprofloxacin is almost perpendicular to the basic structure (Figure 4b and Table 2). The conformation is shaped like a lollipop, and thus the ciprofloxacin antibody should be able to accommodate a large group and demonstrated a broad specificity according to the QSAR analysis above in this study. Actually, this was also verified again by a previously reported monoclonal antibody and a developed broad-specificity immunoassay for 12 quinolones (Table S5).<sup>18</sup> The conformations of norfloxacin and sarafloxacin in the fourth group were also like the letter Y and were similar to that of ciprofloxacin. As a result, their antibodies also would show broad specificity similarly to ciprofloxacin. The numbers of structurally related quinolones of norfloxacin and sarafloxacin whose cross-reactivity values were over 15% were 13 and 10, respectively (Table S5).<sup>9,31</sup>

Therefore, it can be concluded that a shape like the letter I, P, or  $\Phi$  is the essential conformational feature of a quinolone hapten used to produce an antibody with high specificity, whereas the conformation of a quinolone hapten with a Y shape (or a lollipop) could be used to produce antibodies with broad specificity.

## ■ CONCLUSIONS

In summary, 3D QSAR studies were performed to investigate the molecular recognition between the antibody and quinolone drugs. The CoMFA model revealed that quinolones shaped like the letters I, P, and  $\Phi$  formed flat conformations that could not accommodate large groups, and thus, the resultant antibodies would have high specificity. In contrast, the hapten conformations shaped like the letter Y lead to antibodies with broad specificity and high cross-reactivity. Almost all of the antibodies against quinolone could result from these four hapten conformations. This finding is the first time to systematically and effectively elucidate and predict the high specificity of quinolone antibodies. It will be of significance for accurate hapten design, predictable antibody specificity, and better understanding of the recognition mechanism of haptens and specific antibodies.

## ■ ASSOCIATED CONTENT

### Supporting Information

The Supporting Information is available free of charge on the ACS Publications website at DOI: 10.1021/acs.analchem.7b00997.

Description of the optimized ciELISA conditions; summary of the calculated parameters of the CoMFA model; predicted values derived from the CoMFA models of pipemidic acid; predicted values derived



from the CoMFA models of clinafloxacin; review of immunoassay for the determination of quinolones in recent years; UV spectra of BSA, OVA, pipemidic acid, pipemidic acid-BSA, and pipemidic acid-OVA; SDS-PAGE pattern obtained using purified pipemidic acid polyclonal antibody; and scatter plots of predicted versus experimental  $pIC_{50}$  values (PDF)

## AUTHOR INFORMATION

### Corresponding Author

\*Phone: +8620-8528 3448. Fax: +8620-8528 0270. E-mail: hongtao@scau.edu.cn.

### ORCID

Zhanhui Wang: 0000-0002-0167-9559

Hongtao Lei: 0000-0002-1697-1747

### Author Contributions

<sup>‡</sup>J.C. and L.W. contributed equally to this work.

### Notes

The authors declare no competing financial interest.

## ACKNOWLEDGMENTS

This work was supported by the Natural Science Foundation of China (U1301214, 30700663, 21475047 and 31601555), Guangdong and Guangzhou Planned Program in Science and Technology (S2013030013338, 2016201604030004, 2014TX01N250, 2013B051000072, and 2014A030306026), Guangdong Natural Science Foundation (2015A030313366), and Guangzhou University of Chinese Medicine (2016KYDT04 and 2016KYDT06).

## REFERENCES

- (1) Van Bambeke, F.; Michot, J. M.; Van Eldere, J.; Tulkens, P. M. *Clin. Microbiol. Infect.* **2005**, *11*, 256–280.
- (2) Andriole, V. T. *Clin. Infect. Dis.* **2005**, *41*, S113–S119.
- (3) Mehlhorn, A. J.; Brown, D. A. *Ann. Pharmacother.* **2007**, *41*, 1859–1866.
- (4) Hernández-Arteseros, J.; Barbosa, J.; Compano, R.; Prat, M. J. *Chromatog. A* **2002**, *945*, 1–24.
- (5) Cañada-Cañada, F.; Espinosa-Mansilla, A.; Jiménez Girón, A.; Muñoz de la Peña, A. *Czech J. Food Sci.* **2012**, *30*, 74–82.
- (6) Pecorelli, I.; Galarini, R.; Bibi, R.; Floridi, A.; Casciarri, E.; Floridi, A. *Anal. Chim. Acta* **2003**, *483*, 81–89.
- (7) Chang, C. S.; Wang, W. H.; Tsai, C. E. *J. Food Drug Anal.* **2010**, *18*, 87–97.
- (8) Dorival-García, N.; Zafra-Gómez, A.; Cantarero, S.; Navalón, A.; Vilchez, J. *Microchem. J.* **2013**, *106*, 323–333.
- (9) Huet, A. C.; Charlier, C.; Tittlemier, S. A.; Singh, G.; Benrejeb, S.; Delahaut, P. *J. Agric. Food Chem.* **2006**, *54*, 2822–2827.
- (10) Lu, S. X.; Zhang, Y. L.; Liu, J. T.; Zhao, C. B.; Liu, W.; Xi, R. M. *J. Agric. Food Chem.* **2006**, *54*, 6995–7000.
- (11) Sheng, W.; Xia, X. F.; Wei, K. Y.; Li, J.; Li, Q. X.; Xu, T. *J. Agric. Food Chem.* **2009**, *57*, 5971–5975.
- (12) Wang, Z. H.; Kai, Z. P.; Beier, R. C.; Shen, J. Z.; Yang, X. L. *Int. J. Mol. Sci.* **2012**, *13*, 6334–6351.
- (13) Cui, J. L.; Zhang, K.; Huang, Q. X.; Yu, Y. Y.; Peng, X. Z. *Anal. Chim. Acta* **2011**, *688*, 84–89.
- (14) Zhang, H. Y.; Wang, S.; Fang, G. Z. *J. Immunol. Methods* **2011**, *368*, 1–23.
- (15) Li, Y. F.; Sun, Y. M.; Beier, R. C.; Lei, H. T.; Gee, S.; Hammock, B. D.; Wang, H.; Wang, Z.; Sun, X.; Shen, Y. D.; Yang, J. Y.; Xu, Z. L. *TrAC, Trends Anal. Chem.* **2017**, *88*, 25–40.
- (16) Leivo, J.; Lamminmäki, U.; Lövgren, T.; Vehniäinen, M. *J. Agric. Food Chem.* **2013**, *61*, 11981–11985.
- (17) Cao, L. M.; Kong, D. X.; Sui, J. X.; Jiang, T.; Li, Z. Y.; Ma, L.; Lin, H. *Anal. Chem.* **2009**, *81*, 3246–3251.
- (18) Wang, Z.; Zhu, Y.; Ding, S.; He, F.; Beier, R. C.; Li, J.; Jiang, H.; Feng, C.; Wan, Y.; Zhang, S.; Kai, Z.; Yang, X.; Shen, J. *Anal. Chem.* **2007**, *79*, 4471–4483.
- (19) Xu, Z.-L.; Shen, Y.-D.; Zheng, W.-X.; Beier, R. C.; Xie, G.-M.; Dong, J.-X.; Yang, J.-Y.; Wang, H.; Lei, H.-T.; She, Z.-G.; Sun, Y.-M. *Anal. Chem.* **2010**, *82*, 9314–9321.
- (20) Luo, L.; Xu, Z. L.; Yang, J. Y.; Xiao, Z. L.; Li, Y. J.; Beier, R. C.; Sun, Y. M.; Lei, H. T.; Wang, H.; Shen, Y. D. *J. Agric. Food Chem.* **2014**, *62*, 12299–12308.
- (21) Chen, J. H.; Lv, S. W.; Wang, Q.; Xu, Z. L.; Yang, J. Y.; Shen, Y. D.; Wang, H.; Sun, Y. M.; Lei, H. T. *Food Anal. Methods* **2015**, *8*, 1468–1476.
- (22) Page, M.; Thorpe, R. In *The Protein Protocols Handbook*; Walker, J. M., Ed.; Humana Press: Totowa, NJ, 2002; p 983–984.
- (23) Oubiña, A.; Barceló, D.; Marco, M. P. *Anal. Chim. Acta* **1999**, *387*, 267–279.
- (24) Yuan, Y. L.; Hua, X. D.; Li, M.; Yin, W.; Shi, H. Y.; Wang, M. H. *RSC Adv.* **2014**, *4*, 24406–24411.
- (25) Yu, F. Y.; Vdovenko, M. M.; Wang, J. J.; Sakharov, I. Y. *J. Agric. Food Chem.* **2011**, *59*, 809–813.
- (26) Chen, J. H.; Lu, N.; Shen, X.; Tang, Q. S.; Zhang, C. J.; Xu, J.; Sun, Y. M.; Huang, X. A.; Xu, Z. L.; Lei, H. T. *J. Agric. Food Chem.* **2016**, *64*, 2772–2779.
- (27) Mu, H. T.; Lei, H. T.; Wang, B. L.; Xu, Z. L.; Zhang, C. J.; Ling, L.; Tian, Y. X.; Hu, J. S.; Sun, Y. M. *J. Agric. Food Chem.* **2014**, *62*, 7804–7812.
- (28) Zhang, H. T.; Jiang, J. Q.; Wang, Z. L.; Chang, X. Y.; Liu, X. Y.; Wang, S. H.; Zhao, K.; Chen, J. S. *J. Zhejiang Univ., Sci., B* **2011**, *12*, 884–891.
- (29) Han, D.; Yu, M.; Knopp, D.; Niessner, R.; Wu, M.; Deng, A. P. *J. Agric. Food Chem.* **2007**, *55*, 6424–6430.
- (30) Lei, H. T.; Su, R.; Haughey, S. A.; Wang, Q.; Xu, Z. L.; Yang, J. Y.; Shen, Y. D.; Wang, H.; Jiang, Y. M.; Sun, Y. M. *Molecules* **2011**, *16*, 5591–5603.
- (31) Jiang, W. X.; Wang, Z. H.; Beier, R. C.; Jiang, H. Y.; Wu, Y. N.; Shen, J. Z. *Anal. Chem.* **2013**, *85*, 1995–1999.
- (32) Liu, Z. Q.; Lu, S. X.; Zhao, C. H.; Ding, K.; Cao, Z. Z.; Zhan, J. H.; Ma, C.; Liu, J. T.; Xi, R. M. *J. Sci. Food Agric.* **2009**, *89*, 1115–1121.
- (33) Li, C.; Jiang, J.; Qi, X. H. In *2011 Eighth International Conference on Fuzzy Systems and Knowledge Discovery (FSKD)*; IEEE Press: Piscataway, NJ, 2011; Vol. 3, pp 1446–1449.
- (34) Zeng, H. J.; Yang, R.; Liu, B.; Lei, L. F.; Li, J. J.; Qu, L. B. *J. Pharm. Anal.* **2012**, *2*, 214–219.
- (35) Zhao, C. B.; Liu, W.; Ling, H. L.; Lu, S. X.; Zhang, Y. L.; Liu, J. T.; Xi, R. M. *J. Agric. Food Chem.* **2007**, *55*, 6879–6884.
- (36) Zhao, Y. L.; Zhang, G. P.; Liu, Q. T.; Teng, M.; Yang, J. F.; Wang, J. H. *J. Agric. Food Chem.* **2008**, *56*, 12138–12142.
- (37) Zhi, A. M.; Li, B. B.; Liu, Q. T.; Hu, X. F.; Zhao, D.; Hou, Y. Z.; Deng, R. G.; Chai, S. J.; Zhang, G. P. *Food Agric. Immunol.* **2010**, *21*, 335–345.